Supporting Information

Non-linear optical response in anisotropic Sb_2Se_3 nanorods suspension and their photonic device applications

Nabanita Sen[a], Nabamita Chakraborty[a], Biswajit Das[a] and Kalyan Kumar Chattopadhyay[a,b*]

[a]*Thin Film and NanoScience Laboratory, Department of Physics, Jadavpur University, Kolkata, 700032, India*

[b]*School of Materials Science & Nanotechnology, Jadavpur University, Kolkata-700032, India*

**Corresponding author's email id: kalyan_chattopadhyay@yahoo.com, kkc.juphy@gmail.com*

Calculation of N_{eff}:

The number of effective layers is estimated in the following based on the calculation of [1]

Total number of molecules in solution of cuvette of volume V, is $N_{tot} = \rho * V * N_A$

Where, ρ = concentration of the solution in mol/L,

V = volume of the cuvette in L, N_A= Avogadro's number ($6.023*10^{23}$)

There are four effective number of molecules per unit cell of Sb_2Se_3 so,

Total number of unit cell of Sb_2Se_3 in solution of cuvette of volume V, is $N_{unit} = N_{tot}/4$.

Thus, a single effective layer contains, m = S/(a*c) unit cell.

Where, S = area of the plane of the cuvette which is perpendicular to the direction of light propagation in cm^2. (a = 11.63 A°, b = 3.97 A°, c = 11.78 A°, are the lattice constant of Sb_2Se_3). Then the layer number is $N_{cell} = N_{unit} / m$. The number of charge carrier layers that the incident laser beam encounter is $N_{eff} = 2* N_{cell}$. (there are two effective charge carrier layers per unit cell).

Third order optical susceptibilities of reported materials.

Materials	Dimensions	Solvent	Concentrations	Laser parameters	$\chi^3_{monolayer}$	References
$MoSe_2$	2D	NMP	$7.1*10^{-4}$mol/L	532 nm CW Laser	10^{-9} e.s.u	2
MoS_2	2D	Acetone	0.14g/L	532 nm CW Laser,400 nm and 800 nm ultrafast lasers	10^{-9} e.s.u	3
$MoTe_2$	2D	NMP	0.1g/L	473 nm,532nm, 750 nm and 801 nm CW Lasers	10^{-9} e.s.u	4
Black phosphorus	2D	NMP	$4.03*10^{-3}$mol/L	350- 1160 nm femtosecond Lasers	10^{-8} e.s.u at multiple wavelengths.	5
Graphite	3D	NMP	0.075mg/L	532 nm CW Laser	$2.2*10^{-9}$ e.s.u	6
Graphene	2D	NMP	-	532 nm CW Laser	10^{-7} e.s.u	7
$Ti_3C_2T_x$	2D	-	-	800 nm femtosecond Laser and 1064 nm picosecond Laser	10^{-15} e.s.u at 800 nm and 10^{-7} e.s.u at 1064 nm	8
TaAS	3D	NMP	0.2g/L	532 nm laser	$9.9*10^{-9}$ e.s.u	1
Te NTs	1D	-	0.25mg/mL	532nm laser	-	9
Te@ BiQDNTs	1D@0D	-	0.25mg/mL	532nm laser	-	9
Sb_2Se_3	1D	NMP	0.25mg/mL	671 nm laser	$1.05*10^{-9}$e.s.u	This Work

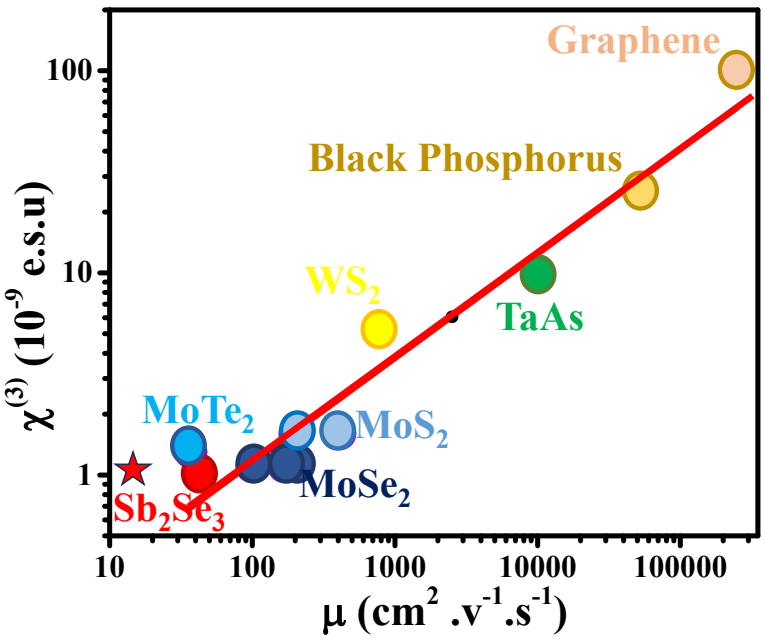

Figure S1. Linear relation between $\chi^{(3)}_{\text{single layer}}$ and carrier mobility μ for 2D layered materials, 3D TaAs and Sb_2Se_3 Red star and red circle depict electron and hole mobility of Sb_2Se_3 respectively. All the values of $\chi^{(3)}$except Sb_2Se_3 are adapted from ref[3],[4],[6],[8],[10]. All the values of μ are adapted from ref [11-21].

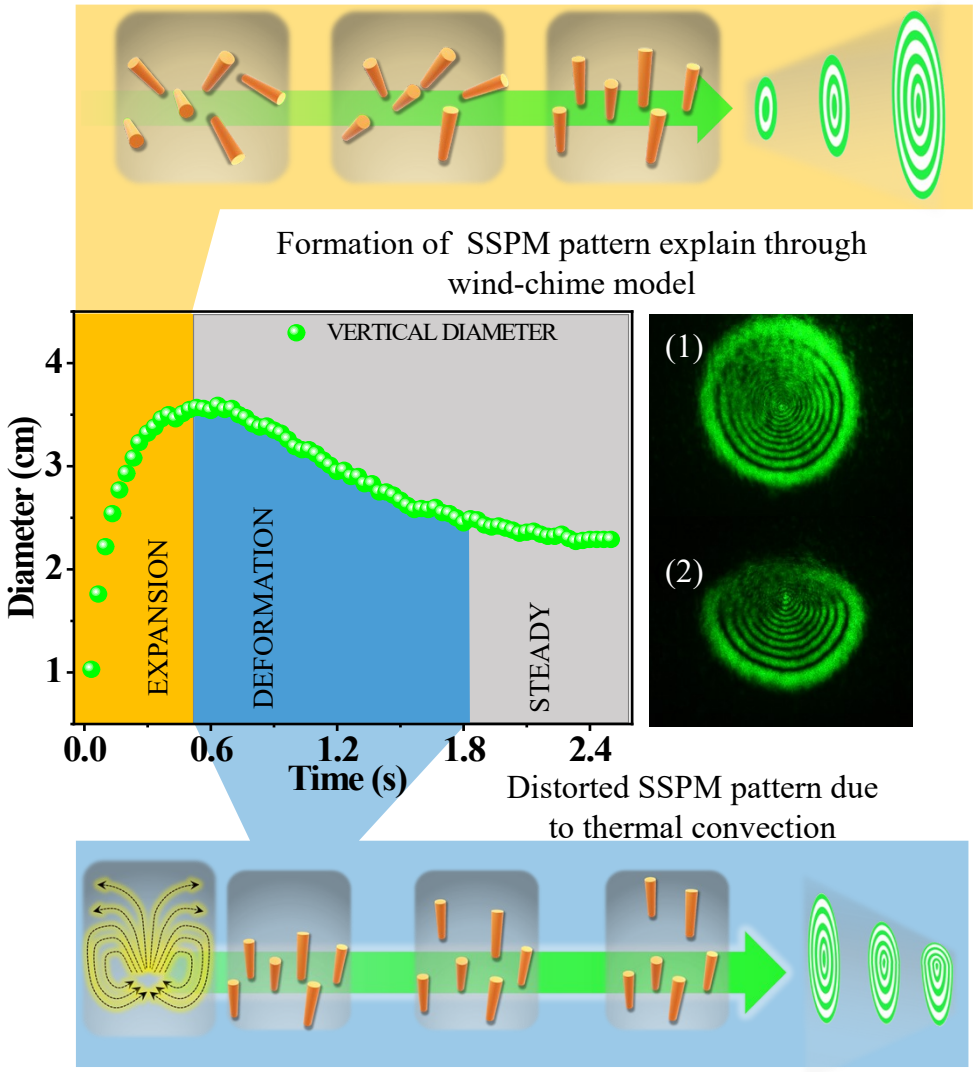

Figure S2. Formation and distortion of SSPM pattern through wind-chime model and thermal convection respectively

Formation of SSPM pattern: As the laser light passed through the sample, diffraction rings appeared and continued to increase in size. This was due to the reorientation of Sb2Se3 nanomaterials layers. The process occurred as follows: when the laser hit the material, electrons and holes were excited and moved in opposite directions, causing polarization of the layered nanomaterial. This polarization caused the layered structure to realign itself parallel to the electric field to minimize the system's energy. The time taken for the diffraction rings to form is equal to the time required for the layered nanomaterial to reorient itself. The formation time of the diffraction rings is dependent on several factors, including the size and permittivity of the material, the viscosity of the solvent, and the intensity of the incident laser light. This wind chime model provides a clear understanding of the formation process.

Distortion of SSPM pattern: Once the diffraction ring reaches its maximum diameter, the upper half of the ring becomes distorted due to thermal convection. As laser light passes through the solvent, it heats the liquid, creating a vertical thermal convection. This convection causes a decrease in the effective nonlinear refractive index n2 in the lower region, resulting in a lower number of polarized Sb2Se3 molecules in the lower part compared to the upper part. The distortion area of the SSPM pattern is opposite to the refractive index distribution. As a result, the upper part of the diffraction rings becomes distorted compared to the lower part.

References

1. Huang, Yixuan, et al. "Laser-Induced Hole Coherence and Spatial Self-Phase Modulation in the Anisotropic 3D Weyl Semimetal TaAs." *Advanced Materials* 35.11 (2023): 2208362.

2. Wang GZ, Zhang SF, Zhang XY, et al. Tunable nonlinear refractive index of two-dimensional MoS_2, WS_2, and $MoSe_2$ nanosheet dispersions. Photonics Res 2015;A51–5.

3. Wu, Yanling, et al. "Emergence of electron coherence and two-colour all-optical switching in MoS2 based on spatial self-phase modulation." *Proceedings of the National Academy of Sciences* 112.38 (2015): 11800-11805.
4. Hu, Lili, et al. "Nonlinear optical response spatial self-phase modulation in MoTe 2: correlations between χ (3) and mobility or effective mass." *Optics Letters* 44.21 (2019): 5214-5217.
5. Zhang, Jingdi, et al. "Broadband spatial self-phase modulation of black phosphorous." *Optics letter* 41.8 (2016): 1704-1707.
6. Wu YL, Zhu LL, Wu Q, et al. electronic origin of spatial selfphase modulation: Evidenced by comparing graphite with C60 and graphene. Appl Phys Lett 2016; 108:241110.
7. Wu R, Zhang YL, Yan SC, et al. Purely coherent nonlinear optical response in solution dispersions of graphene sheets. NanoLett. 2011; 11:5159–64.
8. Li, Jie, et al. "Broadband spatial self-phase modulation and ultrafast response of MXene Ti3C2Tx (T= O, OH or F)." *Nanophotonics* 9.8 (2020): 2415-2424.
9. Wu, Leiming, et al. "1D@ 0D hybrid dimensional heterojunction-based photonics logical gate and isolator." *Applied Materials Today* 19 (2020): 100589.
10. Gaozhong Wang, Saifeng Zhang, Xiaoyan Zhang, Long Zhang, Ya Cheng, Daniel Fox, Hongzhou Zhang, Jonathan N. Coleman, Werner J. Blau, and Jun Wang. photonics research,**2015,**3 A51-A55.
11. L. Cheng and Y. Y. Liu, J. Am. Chem. Soc. 140, 17895 (2018).
12. S. V. Morozov, K. S. Novoselov, M. I. Katsnelson, F. Schedin, D. C. Elias, J. A. Jaszczak, and A. K. Geim, Phys. Rev. Lett. 100, 016602(2008).

13. M. Orlita, C. Faugeras, P. Plochocka, P. Neugebauer, G. Martinez, D. K. Maude, A.-L. Barra
M. Sprinkle, C. Berger, W. A. de Heer, and M. Potemski, Phys. Rev. Lett. 101, 267601 (2008).
14. S. L. Li, K. Tsukagoshi, E. Orgiu, and P. Samorı, Chem. Soc. Rev. 45, 118 (2016).
15. S. Das, H.-Y. Chen, A. V. Penumatcha, and J. Appenzeller, Nano Lett. 13, 100 (2013).
16. M. M. Perera, M.-W. Lin, H.-J. Chuang, B. P. Chamlagain, C. Wang, X. Tan, M. M.-C. Cheng, D. Tomanek, and Z. Zhou, ACS Nano 7, 4449(2013).
17. N. R. Pradhan, D. Rhodes, Y. Xin, S. Memaran, L. Bhaskaran, M. Siddiq, S. Hill, and L. Balicas, ACS Nano 8, 7923 (2014).
18. N. R. Pradhan, D. Rhodes, S. Feng, Y. Xin, S. Memaran, B.-H. Moon, H. Terrones, M. Terrones, and L. Balicas, ACS Nano 8, 5911 (2014).
19. I. G. Lezama, A. Ubaldini, M. Longobardi, E. Giannini, C. Renner, A. B. Kuzmenko, and A. F. Morpurgo, 2D Mater. 1, 021002 (2014).
20. G. Long, D. Maryenko, J. Y. Shen, S. G. Xu, J. Q. Hou, Z. F. Wu, W. K. Wong, T. Y. Han, J. X. Z. Lin, Y. Cai, R. Lortz, and N. Wang, Nano Lett. 16, 7768 (2016)
21. K. Zeng, D. J. Xue and J. Tang. Antimony Selenide Thin Film Solar cells. Semicond. Sci. Technol. **2016**, 31, 063001.